We are IntechOpen, the world's leading publisher of Open Access books Built by scientists, for scientists

6,900
Open access books available

185,000
International authors and editors

200M
Downloads

Our authors are among the

154
Countries delivered to

TOP 1%
most cited scientists

12.2%
Contributors from top 500 universities

WEB OF SCIENCE™

Selection of our books indexed in the Book Citation Index in Web of Science™ Core Collection (BKCI)

Interested in publishing with us?
Contact book.department@intechopen.com

Numbers displayed above are based on latest data collected.
For more information visit www.intechopen.com

Chapter 5

Multiphoton and Fluorescence Lifetime Imaging Microscopy in Studying Nanoparticle Pharmacokinetics in Skin and Liver

Camilla A. Thorling, Amy Holmes, Hauke Studier, David Liu, Xiaowen Liang and Michael S. Roberts

Additional information is available at the end of the chapter

http://dx.doi.org/10.5772/63452

Abstract

The use of nanoparticles has increased in consumer products in recent decades; however, concerns regarding their safety remain. Zinc oxide is used in sunblocking and may generate free radicals in response to UV illumination, leading to DNA damage and an immunological response. With high-resolution, high-contrast imaging in biological tissue, multiphoton microscopy is able to separate nanoparticles signals from endogenous fluorophores. It has been proven to be very useful in imaging penetration of zinc oxide nanoparticles in skin and in combination with fluorescence lifetime imaging microscopy study cellular function as well. This chapter aims to review the use of these imaging techniques in studying the uptake and distribution of nanoparticles in skin and liver. Due to the questionable clinical use and possible toxicity of nanoparticles, it is important to study their pharmacokinetics. Some nanomaterials have been identified as relatively toxic to humans and a few metal nanoparticles have been reported to penetrate and be detected in blood. Multiphoton microscopy has high resolution and is able to visualize nanoparticles, due to their optical properties, *in vivo*. The addition of fluorescence lifetime imaging makes it possible to measure the physiochemical environment, with outputs that can be statistically analyzed, posing an advantage over fluorescence intensity imaging only.

Keywords: multiphoton microscopy, fluorescence lifetime imaging microscopy, nanoparticles, skin, liver

INTECH
open science | open minds

© 2016 The Author(s). Licensee InTech. This chapter is distributed under the terms of the Creative Commons Attribution License (http://creativecommons.org/licenses/by/3.0), which permits unrestricted use, distribution, and reproduction in any medium, provided the original work is properly cited. CC BY

1. Introduction

Nanoparticles (NPs) are particles ranging from 1 to 100 nm in size and are a promising pharmaceutical tool for drug delivery and functionalized cosmetic products like sunscreens. There are growing public and regulatory concerns of topical application of NPs, due to the increasing manufacturing of NPs in commercial products as well as continuing discovery of new applications. NPs are available in several different shapes, such as sphere, rod, cylinder, and cube. Furthermore, they can be soft or hard, aggregated or dispersed. NPs present in commercial products are often made from metals such as gold and silver or metal oxides like zinc oxide and titanium oxide, but also include quantum dots (QDs), carbon nanotubes, fullerenes, and lipid-based materials. From an environmental and occupational health and safety point of view, it is important to investigate NPs interaction with organs following unintended exposure. On the other hand, it is very necessary to study their properties in active drug delivery and clearance without adverse effects for therapeutic and cosmetic applications. Properties, such as particle size and shape, surface charge, pH, formulation, are important factors in determining the penetration of NPs in the skin. Toxicity of NPs is mainly of concern for the smaller particles. The skin may be more susceptible to NPs penetration if it is diseased, hot, damaged, inflamed, hydrated, dry, or moisturized. Positively charged NPs are most preferred for skin penetration [1].

Determining the presence or absence as well as concentration of NPs in biological tissue has been enabled by multiphoton microscopy (MPM), especially in investigating interactions of NPs with human skin [2].

Most knowledge in the biological world has been gathered from studying images [3]. Thus, a growing interest for live-tissue imaging has evolved. In conventional confocal microscopy, the intensity from the beam is approximately uniform above and below the focal plane, which results in the specimen generating fluorescence out of the focal plane that is rejected by the pinhole. This leads to the specimen being subjected to photobleaching and photodamage, affecting image quality, and tissue health [4]. MPM avoids this because a much smaller area of the specimen is being stimulated by the excitation light source and no out of focus light is generated, which leads to photobleaching being restricted to the focal point only [4, 5]. At an excitation wavelength in the near infrared range (NIR, ~ 700–1000 nm), the photon penetration depth of the incident light is maximized, and the tissue scattering and absorption are minimized [6, 7].

In confocal microscopy (single photon), fluorescence occurs when a photon is absorbed by a fluorescent molecule and raises an electron to an excited energy state (**Figure 1**). When the electron returns to the ground state, it converts the absorbed energy to heat, by transferring the energy to another molecule emitting a lower energy photon [8, 9], producing an image. In MPM, two (or more) photons of the same energy from a pulsed laser (usually femtosecond laser) interact with a molecule to produce excitation equivalent to the absorption of a single photon possessing twice (or multiple) the energy (**Figure 1**). If the excited molecule is fluorescent, it can emit a single photon [8–10].

http://dx.doi.org/10.5772/63452

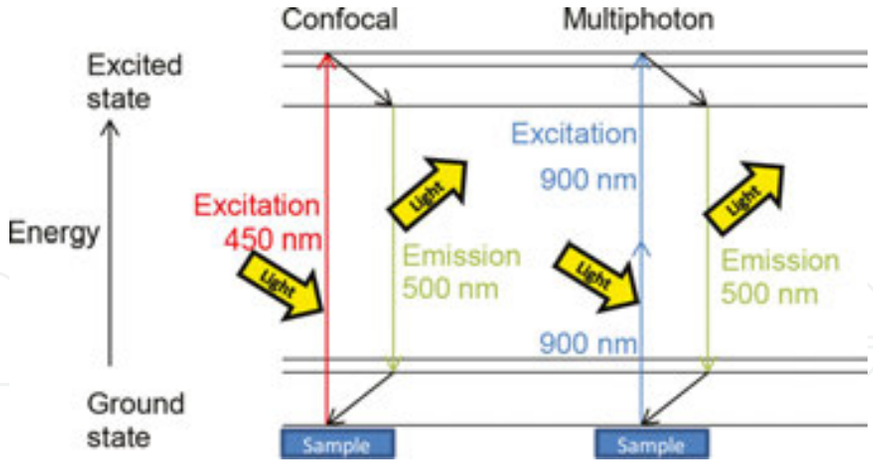

Figure 1. Jablonski energy diagram (adapted from Refs. [8–11]). Imagine a fluorescent molecule with single absorption and emission at 450 and 500 nm, respectively. In order to excite electron(s) from this molecule, light from a laser is needed. The electron(s) is then raised into a higher excited state, where it decays rapidly into the ground vibrational state within the electronically excited state. From there the electron can return to the electronically ground state by emitting light, which can yield in fluorescence. The emitted light has lower energy (higher wavelength) than the absorbed light. The emission spectrum of fluorescence excited by MPM is usually similar to the one excited with single photon excitation. To excite the molecule with two-photon, two photons of equal wavelengths, which together meet the energy gap between the ground and excited states, are needed (here 900 nm).

An important application of MPM is to image the physiology, morphology, and cell-cell interactions in intact tissue of live animals with high resolution. However, one limitation is that it cannot quantitatively study cellular function on a molecular level [12]. MPM in combination with fluorescence lifetime imaging microscopy (FLIM), however, can identify fluorophores with overlapping spectral properties. Furthermore, it enables insights into their biological function by being sensitive to the binding site and the environmental surrounding [13]. The fluorescence lifetime is proportional to the reciprocal Einstein coefficient of the spontaneous emission, that is, to the sum of the rate constants of all possible return paths for the electron from the excited state to the ground state that is not stimulated emission [14]. This is determined by both intramolecular and intermolecular events [4]. FLIM has been described as a direct approach to monitor energy transfers between fluorophore and the environment, for example, DNA binding, which change the fluorescence lifetime of that fluorophore [15]. FLIM is particularly important when identifying fluorophores with overlapping spectral properties [13]. One application for FLIM in liver imaging is to study levels of the autofluorescent NADH, as a direct measure for the redox state as a metabolic marker of the cells [8].

The principle of FLIM is illustrated in **Figure 2**. Imagine a sample with two regions, each with equal intensity, but two different fluorescence lifetimes, one shorter ($\tau 1$) and one longer ($\tau 2$). $\tau 2$ could be due to binding to other molecules, change in pH, cation concentration, oxygen concentration, or polarity. The intensity image itself can not reveal these environmental differences (**Figure 2a**), but the FLIM image can (**Figure 2b** and **c**). The fluorescence lifetimes within a FLIM image can be presented on a grey (**Figure 2b**) or colour scale (**Figure 2c**) or as

three-dimensional (3D) surface where the height represents the local decay times (**Figure 2d**) [16].

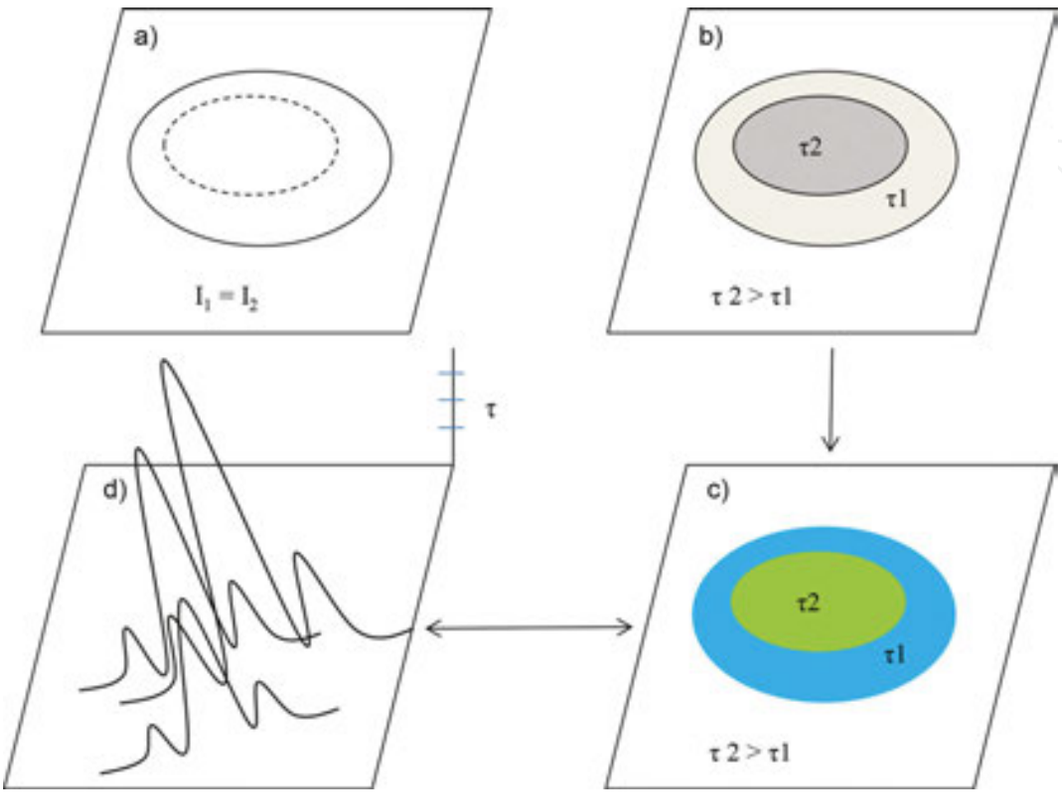

Figure 2. Principles of fluorescence lifetime imaging (FLIM). (a) Intensity (I) cannot reveal any difference in the surrounding environment; (b) FLIM enables distinguishing the two components with different fluorescence lifetime and can give insights into biological function (grey scale represents fluorescence lifetimes, where τ2 > τ1). (c) Fluorescence lifetimes can also be colour coded or; (d) displayed as third coordinate, resulting in a 3D image (adapted from Ref. [Lakowitz et al., Fluorescence lifetime imaging of free and protein-bound NADH. *Proceedings of the National Academy of Sciences* 1992 89(4): 1271-1275).

MPM can be used to image fluorescent and sometimes even nonfluorescent NPs in living cells, tissue, and organs *in vivo*. Nonfluorescent NPs can have nonlinear optical properties so that they can become visible for MPM (e.g., zinc oxide (ZnO) NPs, gold (Au) NPs, and silver (Ag) NPs) [17]. One physical phenomenon is second harmonic generation (SHG). It is based on elastic scattering. The wavelength of the SHG signal is at the double frequency of the incident excitation light of the femtosecond laser. The optical response is quasi-instantaneous and therefore can easily be identified by FLIM. A second process is the so-called localized surface plasmon resonance (LSPR) [18]. The LSPR signal can be tailored by modifying the size or the shape of the NPs. This signal can be very broadband (inelastic phenomenon) and strong but is also characterized by a very rapid optical response in the femtosecond range so that it also can easily be identified by FLIM technique [19].

MPM has proven to be very useful in imaging the uptake of metal NPs, such as ZnO-NPs, Au-NPs and Ag-NPs in the skin. Additionally, NAD(P)H (NADH+NADPH) can be imaged

http://dx.doi.org/10.5772/63452

simultaneously without the need for additional dyes using FLIM. This can help to understand how NPs affect the viable skin condition. The additional time-resolved measurements with FLIM can be used to differentiate NP signals from endogenous tissue [2]. This chapter aims to critically review the use of these imaging techniques in studying the penetration of NPs and quantum dots (QDs) into skin, how to facilitate intentional uptake, as well as the uptake and distribution in the liver.

2. Topical application of zinc oxide nanoparticles

Zinc oxide NPs (ZnO NPs) are incorporated into a plethora of commercially available formulations including sunscreens, cosmetics such as mineral-based make-up, and nappy rash ointments. Though ZnO NPs are considered to be safe after topical application [20], there have been concerns raised about the lack of assessment of toxicity under "in-use" conditions [21]. ZnO NPs are transparent and affords the viable epidermis broad spectrum protection from harmful UV radiation. Irradiation of ZnO NPs, however, can result in the production of reactive oxygen species (ROS) that are harmful if exposed to the keratinocytes within the viable epidermis [22]. It is therefore of importance to delineate the deposition of ZnO NPs after topical application to comprehensively assessing whether ZnO NPs can penetrate the stratum corneum and reach the viable epidermis. A ZnO NP suspension was applied to human skin *in vivo* at 10% wt for 6 hours and then occluded to simulate clothing covering the skin with the applied sunscreen. It was found that occlusion, and thus, skin hydration does not aid the penetration of ZnO NPs into human skin and no localized toxicity was observed within the viable epidermis using metabolic lifetime imaging [23]. In this study, the photoluminescence of ZnO NPs was spectrally resolved from that of the endogenous fluorophores, and thus, the deposition was mapped after application to the volunteers' forearms. The fluorescence lifetime amplitude, α_1%, of ZnO NPs (multiphoton-excited photoluminescence) was found to be distinct from that of the autofluorescence. This enabled the authors' to map the distribution of ZnO NPs after application to viable skin *in vivo*. Further, using MPM–FLIM, the free-to-bound ratio of endogenous NAD(P)H was determined to elucidate any effect ZnO NP application had on the redox state of the viable epidermis.

Other studies conducted include the *in vivo* application of ZnO NPs with massage and arm flexing in which the conclusions were that again no ZnO NP penetration as observed with the exception of ZnO NPs within the sebaceous gland of one volunteer and no localized toxicity was observed by metabolic imaging [23]. An *in vivo* study was also conducted to assess any ZnO penetration after repeated exposure [25] as the cancer council advises the public to reapply sunscreen every 2 hours [24]. In this study, once again no ZnO NP penetration or localized toxicity within the viable epidermis was observed even after repeated liberal application to volunteers' forearm [25]. Lin et al. applied ZnO NPs to intact human skin and also skin that was tape-stripped (20×), or had psoriatic and atopic dermatitis lesions. The study showed that the ZnO NP photoluminescence signal was most intense at the skin surface after application to impaired lesioned skin compared to intact skin *in vivo*. In this study, no penetration of ZnO NP was observed within the viable epidermis after application of ZnO NPs in caprylic capric triglyceride (CCT) [26].

As NPs have a high surface-to-volume ratio, the reactivity and dissolution of constituent ions increases with decreasing diameter of the NP. Zinc ion release and percutaneous absorption has been observed after topical ZnO NP application to human skin both *in vivo* [27–29] and *in vitro* [30]. Further, NPs are known to accumulate within the hair follicles and undulations of human skin for up to 10 days [31] whereby they may act as a reservoir undergoing dissolution into constituent solubilized species within these reduced environments. To increase stability, reduce dissolution and production of ROS, coated ZnO NPs have been employed within formulations. Leite-Silva et al. [23] investigated the deposition of ZnO NPs after application to *in vivo* human skin within various formulations. MPM–FLIM was used once again to simultaneously map ZnO NP deposition whilst also determining the NAD(P)H free-to-bound ratio of the underlying viable epidermis after application of both coated and uncoated ZnO NPs in (a) CCT suspension, (b) a gel formulation, (c) oil-in-water emulsion, and (d) water-in-oil emulsion. The study reported the deposition of the ZnO NPs only within the superficial layers of the stratum corneum and within the furrows as reported previously after application in a water-in-oil emulsion (Roberts MS, Roberts MJ, Robertson TA, Sanchez W, Thorling CA, Zou Y, Zhao X, Becker W and Zvyagin AV. In vitro and in vivo imaging of xenobiotic transport in human skin and in the rat liver. *Journal of Biophotonics* 1(6): 478-493, 2008). The exception was minimal ZnO NP penetration was observed within isolated areas in parallel to the furrow within the stratum granulosum after application of coated ZnO NPs in a water-in-oil emulsion observed in **Figure 3** [23]. This, however, did not result in a change in redox state within the stratum granulosum; therefore, the penetrated ZnO NPs did not cause toxicity [23].

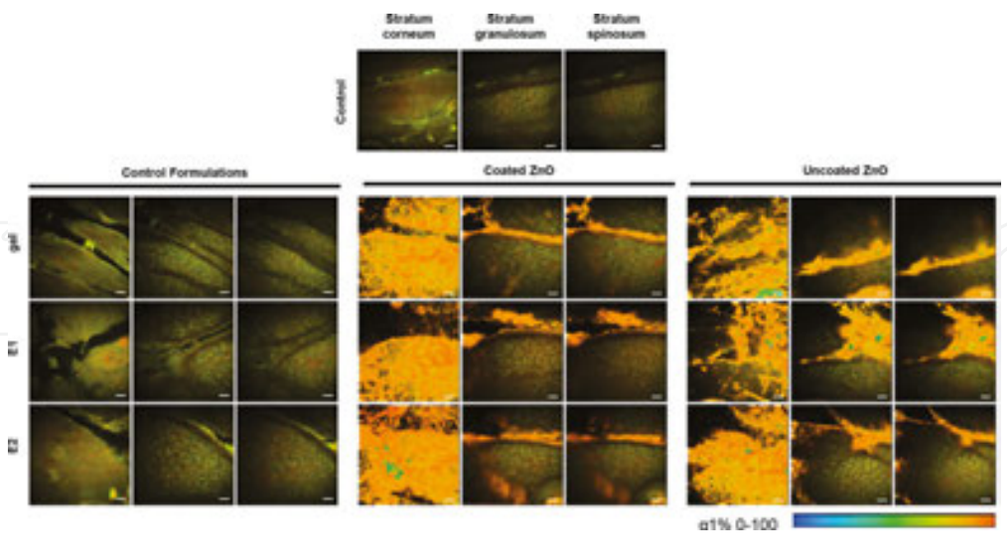

Figure 3. Pseudocoloured MPM–FLIM images of human skin treated with ZnO NPs *in vivo*. ZnO NPs were dispersed in three types of formulations, gel, emulsion E1 o/w, and emulsion E2 w/o in coated or uncoated form. Control images do not contain any NPs. The green colour corresponds to skin autofluorescence (α_1% 45-85), whereas the orange-red colour corresponds to ZnO-NPs photoluminescence (α_1% 90–100). Scale bar is 20 μm. The colour scale bar represents α_1% 0–100.

http://dx.doi.org/10.5772/63452

3. Topical application of gold nanoparticles

Gold NPs (Au NPs) are being increasingly investigated for topical drug delivery due to their monodispersed controllable size, the ability to functionalize the surface of the Au NPs and due to their low reactivity potential. Recently, Au NPs have been investigated as a drug delivery platform in the treatment of psoriasis [32] and as contrast agents in skin cancer imaging [33]. The Au NP (6–15 nm in diameter) penetration study showed 15 nm AuNP in aqueous solution was also observed by MPM–FLIM to aggregate within furrows of skin after treated on excised viable skin sample and also showed penetration of 6 nm Au NP suspended in toluene within the stratum spinosum of the viable epidermis [34]. No change in the redox state of the viable epidermis was observed when Au NPs were applied to the skin in an aqueous vehicle though a change in redox state was observed when Au NPs were applied in toluene [34]. The authors' further investigated the penetration of Au NPs into skin using dimethyl sulfoxide (DMSO), a known chemical penetration enhancer, and found that DMSO enhanced the penetration of Au NPs into skin [35]. A study also showed that Au NP skin penetration was found to be size dependent with 6 nm Au NPs penetrating to higher degree than 15 nm Au NPs [35]. Fernandes et al. found that the skin penetration on Au NPs could be tailored depending on the surface chemistry and shape of the NP [36]. Larese Filon et al. also concluded that Au NPs can penetrate into both intact and impaired human skin *in vitro* [37]. Conversely, Lin et al. found no penetration of Au NPs after topical application to human skin *in vivo* (as shown in **Figure 4**). In this study, Au NPs of increasing diameter 10, 30, and 60 nm were applied to viable *ex vivo* human skin and MPM–FLIM was used to assess any percutaneous absorption of Au NPs. No penetration of Au NPs was observed past the stratum corneum and no change in the redox state of the viable epidermis was observed indicating no localized toxicity [38]. The scientific community has yet to reach a consensus on whether inorganic NPs can penetrate human skin as exhibited by conflicting results within the literature.

4. Topical application of other nanoparticles

SECosomes are flexible nanovesicles constituted from surfactant, ethanol, and cholesterol, hence the name SECosomes. MPM–FLIM was used to observe the penetration of SECosomes into viable *ex vivo* human skin as deep at 40 μm within the viable epidermis, which resulted in a shift of lifetime for NAD(P)H [39]. Silver NPs (Ag NPs) are found within a wide variety of personal care products including deodorants', antibacterial under garments, and wound dressings. To determine whether Ag NPs penetrate human skin *in vivo,* Ag NPs were applied to intact or tape stripped skin. No statistically significant difference in metabolic rate measuring the inverse ratio of free-to-bound NAD(P)H (α_1/α_2) was observed within the viable epidermis [40]. In a more recent study, the shape dependence of Ag NPs and their penetration into human skin was determined on *ex vivo* human skin [19]. No Ag NPs either cube, sphere, or truncated plates were observed within the viable epidermis in intact skin but Ag NP plates were found within the wound bed of burned human skin. In this study, Ag NPs penetration into both intact and burned human skin was assessed through detection of both the second

harmonic generation (SHG) signal and the localized surface plasmon resonance (LSPR) of the NPs. Using MPM–FLIM, the detected nonlinear optical characteristics (SHG and LSPR) found that the Ag NPs accumulated within the furrows of the skin, and in particular, the truncated Ag NP plates showed great substantivity within the superficial layers of the stratum corneum but that no penetration into the viable epidermis was observed for intact skin [19]. The authors' also observed that Ag NP spheres accumulated within and around the hair follicle shafts after topical application. This was also supported by the work of Zhu et al. [41] as they too did not observe any penetration of Ag NPs into the viable epidermis of intact porcine skin but did image Ag NPs within the hair follicles using MPM–FLIM and Raman scattering microscopy.

QDs are 2–10 nm fluorescent semiconductor nanomaterials with a larger excitor Bohr radius than the NP radius, making these nanomaterials to undergo quantum confinement. As a result, QDs have characteristic excitation states and larger bandgap values than bulk materials. Emission wavelengths is dependent on size, bandgap increases as the radius decreases (i.e., for smaller QDs). They have greater resistance to photobleaching and have higher quantum

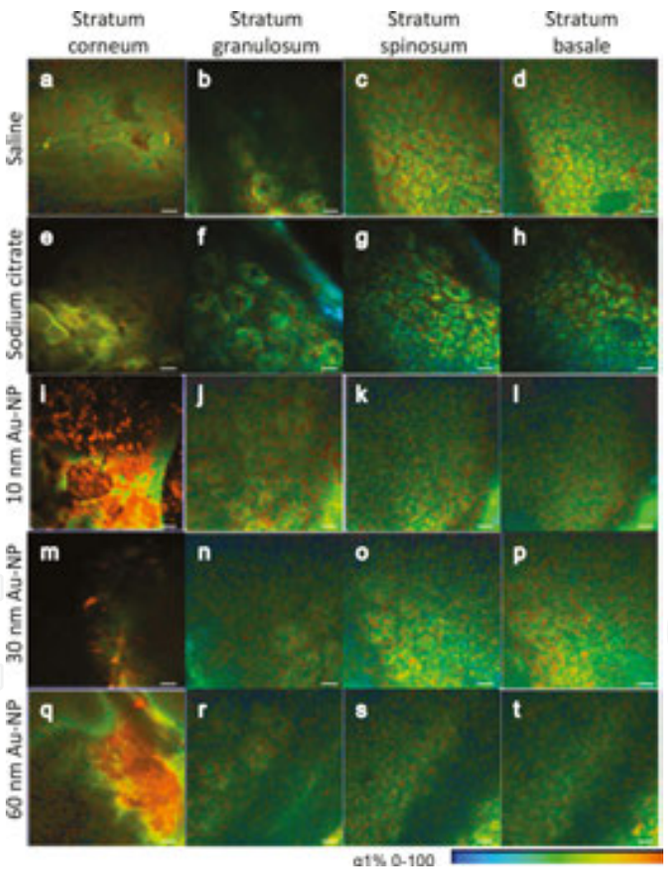

Figure 4. En face MPM–FLIM images of treated human viable skin. FLIM images showing the different layers of excised full-thickness skin (stratum corneum, granulosum, spinosum, and basale) after 24-hour treatment with Au NPs suspended in sodium citrate. Images are pseudocoloured based on α_1% signal (skin autofluorescence 0–95% and AuNPs 95–100% signal). No Au NP signal was detected in the saline control (a)–(d) and detected in the sodium citrate control (e)–(h). The AuNP-treated groups, 10 nm (i)–(l), 30 nm (m)–(p), and 60nm (q)–(t), resulted in signal throughout the stratum corneum. Scale bar indicates 20 μm. Colour bar, blue to red indicates α_1% 0–100%.

http://dx.doi.org/10.5772/63452

yield than conventional fluorophores [42]. Here, they characterized water-soluble cadmium selenide–zinc sulphide quantum dots for MPM imaging in live animals. They visualized QDs dynamically through mice skin in capillaries hundreds of micrometres deep [43].

The advantages that MPM-FLIM provides over other imaging techniques as outlined in the Introduction section have enabled numerous researchers to map the deposition and potential percutaneous absorption of a wide variety of NPs into skin. Further elucidation is required, however, to determine whether NPs can penetrate human skin due to conflicting conclusions within the literature and with the nanotechnology sector rapidly increasing the risk of dermal exposure to NPs will increase.

4.1. How do we improve penetration of nanoparticles for drug delivery?

The penetration of NPs can be improved by penetration enhancers, such as oleic acid, urea, sodium lauryl sulphate, polysorbate, and DMSO. MPM was used to visualize the penetration of a fluorescent NP with the assistance of oleic acid. The results showed that oleic acid was effective in facilitating transdermal delivery of NPs [44]. Au NPs penetration was studied with the chemical enhancers, urea, sodium lauryl sulphate, polysorbate, and DMSO, and it was evident that the penetration was induced by DMSO [35]. Similarly, chemical enhancers can increase penetration of ZnO NPs, by increasing lipid fluidity or by extracting noncovalently bound amphiphilic lipid in the stratum corneum [26].

Another way of increasing penetration of NPs is by using microneedles, which can create pores in the stratum corneum layer, which enables delivery of NPs to the deeper layers of the skin. Gantrez R_AN-139 microneedle successfully did this [45]. Two-photon polymerization of an acrylate-based polymer was used to fabricate microneedle devices for transdermal drug delivery and MPM visualized QDs penetration in porcine skin by a microneedle device [42].

5. Nanoparticles disposition in the liver

NPs are increasingly being used for the detection and treatment of human diseases, in applications such as drug and gene delivery, imaging, and diagnostics [46, 47]. However their short *in vivo* half-lives limit their clinical utility and can lead to hepatotoxicity [46]. It is important to monitor the biodistribution of NPs after intravenous administration in order to evaluate their efficacy and possible side effects. The physiochemical properties of NPs, such as size, shape, surface charge are important in determining the biodistribution [2–5]. For example, hydrophobic NPs are rapidly removed by reticuloendothelial system (RES), mainly by the liver and spleen [46]. Additionally, intravital imaging showed that positively charged NPs where taken up by the hepatocytes (liver cells), whereas negatively charged NPs were found to be taken up by Kupffer cells, liver macrophages, instead [46]. The positively charged NPs have the potential to be cleared via hepatobiliary excretion; however, the negatively charged NPs portends significant hepatotoxicity due to their accumulation in Kupffer cells [46]. If NPs are taken up by hepatocytes, this would be through receptor-mediated endocy-

totic processes [48]. This is in contrast to smaller molecules, such as RH123 and fluorescein, which are taken up by diffusion and transporter proteins in the liver membranes [49].

In a recent study, a multimodal nonlinear label-free imaging technique to pinpoint polymeric NPs within the intestine and liver was done. Encapsulation of active substances within nanoscale particles can enhance bioavailability and biocompatibility, resulting in targeted drug delivery, solubility, and bioactivity and reducing toxicity. They used MPM to show cellular structures, SHG to visualize collagen and CARS to generate chemical-specific images of polymer-based NPs with contrast derived from the molecular vibration of carbon–deuterium bonds within the polymer's palmitic acid chains. These modalities combined give accurate location of the NPs in relation to the cellular structure in the liver, gall bladder, and intestine [50].

The use of MPM to visualize the delivery of Cy5-siRNA with lipid NPs vehicles to hepatocytes was shown by Chen et al. They analysed the diffusion of Cy5-siRNA into the hepatocytes by computation of the percentage signal strength in the region of interest over time [51].

Quantum dots (QDs) are nanomaterials recognized as promising diagnostic and imaging agents. QDs are the most effective semiconductor materials for applications in the field of bioimaging, since they have unique optical and photophysical properties, with high quantum yield and strong fluorescence at both visible and NIR wavelengths. QDs are also stable and retain their fluorescence for a long period of time. QDs have been found to be retained in the organs of the RES for over 22 days after injection, suggesting that they are consumed by mononuclear phagocytes [52]. QDs are particularly well suited for the detection of low abundance antigens, such as hepatitis C virus (HCV), because they are less prone to photobleaching. MPM has been used in combination with QDs to visualize the distribution of HCV-infected cells within the liver [53].

In a previous study, our group applied MPM–FLIM to investigate the *in vivo* subcellular, spatiotemporal disposition of negatively charged QDs in rat liver. The cellular behaviour of QDs was found to be very different from traditional fluorescent molecules, rhodamine 123 (RH123) and fluorescein (**Figure 5**). Results showed that QDs were quickly detected in the liver sinusoids immediately after injection and were not taken up by hepatocytes, but the fluorescence stayed in the sinusoids and started to decrease after about 60 min. The QDs were found to be taken up by Kupffer cells and liver sinusoidal endothelial cells (LSECs).

http://dx.doi.org/10.5772/63452

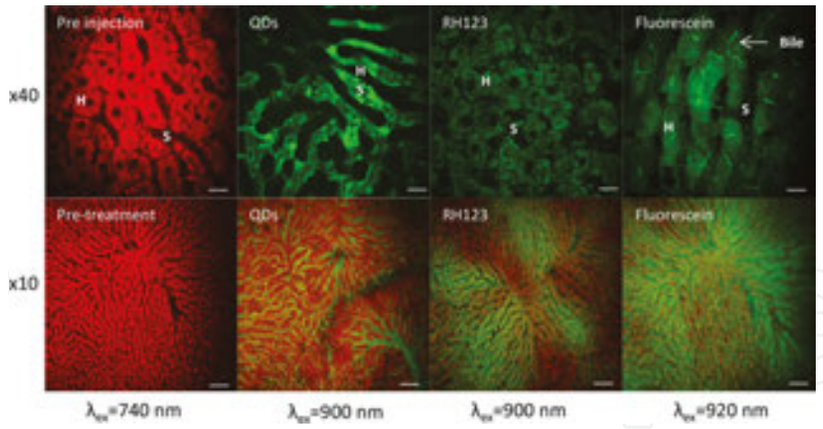

Figure 5. False-coloured images of QDs, RH123, and fluorescein distribution in the rat liver at 5 min after injection (adapted from Ref. [49]) using high (×40) and low (×10) magnification objectives. Red colour represents autofluorescence of the liver excited at 740 nm. Green colour represents the fluorophores, QDs, RH123, and fluorescein, excited at 900 and 920 nm. Scale bar is 20 μm, H = hepatocyte, S = sinusoid, arrow points to bile ducts.

The distribution of these QDs was similar to the distribution of rhodamine B isothiocyanate/dextran 7000, which is a fluorescent marker for labelling the sinusoids of the liver. Additionally, this is in accordance to another study where they found no uptake of negatively charged fluorescein isothiocyanate-labelled mesoporous silica NPs [16]. Both RH123 and fluorescein are excreted through the bile, and hence, the fluorescence signal in the liver declined rapidly, but since these QDs were not excreted through the bile, the fluorescence declined much slower. The fluorescence lifetime of the sinusoids increased after QDs injection, which was due to the long lifetime of QD [49].

Fast and reliable ratiometric FLIM (rmFLIM) approach is described to analyse the distribution of protein-ligand complexes in the cellular context. In combination with Forster resonance energy transfer (FRET), FLIM can be used to map protein–protein interactions on the nanometer-scale in living cells. Organic fluorophores label the ligands in the case of membrane receptors or intracellular proteins that bind extracellular ligands. Imaging based on fluorescence intensity is often used to localize cellular sites where the ligand binds to its cognate receptor, but these techniques may be biased by unspecific binding and distribution of the ligand in various subcellular compartments. FLIM is sensitive to the physiochemical environment, posing an advantage over fluorescence intensity measurements. In this study, they show a fast and reliable FLIM-based method for the localization of target molecules and their discrimination against the fluorescent background of cell membranes and tissue. FRET relies on the shortening of the donor lifetime due to the less energy transfer of radiation to the acceptor. Physiochemical environment can also affect the fluorescence lifetime, for example, quenching. The shortening of fluorescein's fluorescence lifetime when it binds to Cys316 in the opsin molecule results from additional dynamic interaction of the bound dye with the surrounding protein matrix, which functions as a quencher. A ratiometric FLIM (rmFLIM) relies on the specific multiexponential lifetime signature of a protein–ligand complex that is unique compared to the fluorescence lifetime distribution of the background. Only one fluorophore is needed. rmFLIM was used to analyse the fate of a polymer-based nanocarrier

for drug delivery in the metabolic clearance process. They used a polyanionic, dendritic polyglycerolsulfate (dPGS) labelled with a fluorescent indocarbocyanine dye (ICC, spectrally analogue to Cy3). In solution, this nanocarrier had 2 fluorescence lifetimes of 0.27 and 1.1 ns. Paraffin-embedded liver section from rats, previously injected with dPGS-ICC, was used for FLIM measurements [54].

6. Conclusions and future directions

In this chapter, we review the use of MPM and FLIM to visualize the disposition of NPs and QDs in the skin and liver. Nanotechnology and its applications in dermatology and drug delivery have received a growing interest over the past years. Increased applications of NPs have led to an enhanced unintentional skin exposure of NPs and it is therefore important to study when and how NPs penetrate skin. Some conclusions of NP penetrations into skin are as follows: (1) The SC forms an effective barrier to NPs penetration, but smaller-sized NPs are more likely to penetrate. (2) Hair follicles are an important collection site for NPs, and increasingly so when the skin is massaged or flexed. (3) The surface charge and formulation of NPs can affect its penetration.

Negatively charged QDs were found to distribute immediately after injection in the sinusoids of mice livers and accumulated in Kupffer cells and LSECs. Positively charged NPs, however, can be taken up by hepatocytes and subsequently be subjected to biliary excretion. It is important to know where NPs are localized after intravenous injection as these cells are emerging as significant targets for therapies in many liver diseases.

Author details

Camilla A. Thorling[1*], Amy Holmes[2], Hauke Studier[2], David Liu[1], Xiaowen Liang[1] and Michael S. Roberts[1,2]

*Address all correspondence to: c.thorling@uq.edu.au

1 Therapeutics Research Centre, Translational Research Institute, School of Medicine, The University of Queensland, Brisbane, Australia

2 School of Pharmacy and Medical Sciences, The University of South Australia, Adelaide, Australia

http://dx.doi.org/10.5772/63452

References

[1] Liang XW, Xu ZP, Grice J, Zvyagin AV, Roberts MS, Liu X. Penetration of nanoparticles into human skin. Current Pharmaceutical Design. 2013;19(35):6353–66.

[2] Prow TW, Monteiro-Riviere NA, Inman AO, Grice JE, Chen X, Zhao X, et al. Quantum dot penetration into viable human skin. Nanotoxicology. 2012;6(2):173–85.

[3] Eliceiri KW, Rueden C. Tools for visualizing multidimensional images from living specimens. Photochemistry and Photobiology. 2005;81(5):1116–22.

[4] Emptage NJ. Fluorescent imaging in living systems. Current Opinion in Pharmacology. 2001;1(5):521–5.

[5] Stutzmann GE, Parker I. Dynamic multiphoton imaging: a live view from cells to systems. Physiology. 2005;20(1):15–21.

[6] Masters BR, So PT. Confocal microscopy and multi-photon excitation microscopy of human skin in vivo. Optics Express. 2001;8(1):2–10.

[7] Hoover EE, Squier JA. Advances in multiphoton microscopy technology. Nature Photonics. 2013;7(2):93–101.

[8] Roberts MS, Dancik Y, Prow TW, Thorling CA, Lin LL, Grice JE, et al. Non-invasive imaging of skin physiology and percutaneous penetration using fluorescence spectral and lifetime imaging with multiphoton and confocal microscopy. European Journal of Pharmaceutics and Biopharmaceutics. 2011;77(3):469–88.

[9] Oheim M, Michael DJ, Geisbauer M, Madsen D, Chow RH. Principles of two-photon excitation fluorescence microscopy and other nonlinear imaging approaches. Advanced Drug Delivery Reviews. 2006;58(7):788–808.

[10] Helmchen F, Denk W. Deep tissue two-photon microscopy. Nature Methods. 2005;2(12):932–40.

[11] Campagnola PJ, Clark HA, Mohler WA, Lewis A, Loew LM. Second-harmonic imaging microscopy of living cells. Journal of Biomedical Optics. 2001;6(3):277–86.

[12] Niesner RA, Andresen V, Gunzer M. Intravital two-photon microscopy: focus on speed and time resolved imaging modalities. Immunological Reviews. 2008;221(1):7–25.

[13] Yan L, Rueden CT, White JG, Eliceiri KW. Applications of combined spectral lifetime microscopy for biology. Biotechniques. 2006;41(3):249.

[14] Becker W. Fluorescence lifetime imaging–techniques and applications. Journal of Microscopy. 2012;247(2):119–36.

[15] Errington RJ, Ameer-Beg S, Vojnovic B, Patterson LH, Zloh M, Smith PJ. Advanced microscopy solutions for monitoring the kinetics and dynamics of drug–DNA targeting in living cells. Advanced Drug Delivery Reviews. 2005;57(1):153–67.

[16] Lakowicz JR, Szmacinski H, Nowaczyk K, Johnson ML. Fluorescence lifetime imaging of free and protein-bound NADH. Proceedings of the National Academy of Sciences. 1992;89(4):1271–5.

[17] Podlipensky A, Lange J, Seifert G, Graener H, Cravetchi I. Second-harmonic generation from ellipsoidal silver nanoparticles embedded in silica glass. Optics Letters. 2003;28(9):716–8.

[18] Mock J, Barbic M, Smith D, Schultz D, Schultz S. Shape effects in plasmon resonance of individual colloidal silver nanoparticles. The Journal of Chemical Physics. 2002;116(15): 6755–9.

[19] Holmes A M, Lim J, Studier H, S RM. Varying the morphology of silver nanoparticles results in differential toxicity against micro?organisms, human keratinocytes and affects skin deposition. 2016 (unpublished data).

[20] Scientific Committee on Consumer Safety OPINION ON Zinc oxide (Nano Form); 2012, SCCS/1489/12. Available from: http://ec.europa.eu/health/scientific_committees/consumer_safety/docs/sccs_o_137.pdf

[21] Miller G, Sales L. Nano ingredients in sunscreen: the need to regulation. Friends of the Earth 2012. Available from: http://emergingtech.foe.org.au/resources/nano-ingredients-in-sunscreen-the-need-for-regulation/

[22] Graf BW, Chaney EJ, Marjanovic M, De Lisio M, Valero MC, Boppart MD, et al. In vivo imaging of immune cell dynamics in skin in response to zinc-oxide nanoparticle exposure. Biomedical Optics Express. 2013;4(10):1817–28.

[23] Leite-Silva VR, Le Lamer M, Sanchez WY, Liu DC, Sanchez WH, Morrow I, et al. The effect of formulation on the penetration of coated and uncoated zinc oxide nanoparticles into the viable epidermis of human skin in vivo. European Journal of Pharmaceutics and Biopharmaceutics. 2013;84(2):297–308.

[24] Cancer Council Australia. Available from: www.cancer.org.au.

[25] Mohammed Y, Sanchez W, Haridass IN, Pilorget C, Penloup AL, Studier H, Chandrasekaran N, et al. Does repeated topical application of zinc oxide nanoparticles over 5 days result in penetration into human skin in vivo? (unpublished work) 2016.

[26] Lin LL, Grice JE, Butler MK, Zvyagin AV, Becker W, Robertson TA, et al. Time-correlated single photon counting for simultaneous monitoring of zinc oxide nanoparticles and NAD (P) H in intact and barrier-disrupted volunteer skin. Pharmaceutical Research. 2011;28(11):2920–30.

[27] Gulson B, Wong H, Korsch M, Gomez L, Casey P, McCall M, et al. Comparison of dermal absorption of zinc from different sunscreen formulations and differing UV exposure based on stable isotope tracing. Science of the Total Environment. 2012;420:313–8.

http://dx.doi.org/10.5772/63452

[28] Gulson B, McCall M, Korsch M, Gomez L, Casey P, Oytam Y, et al. Small amounts of zinc from zinc oxide particles in sunscreens applied outdoors are absorbed through human skin. Toxicological Sciences. 2010, 118, 140–149.

[29] Ågren M. Percutaneous absorption of zinc from zinc oxide applied topically to intact skin in man. Dermatology. 1990;180(1):36–9.

[30] Holmes AM, Song Z, Moghimi HR, Roberts MS. Relative penetration of zinc oxide and zinc ions into human skin after application of different zinc oxide formulations. ACS Nano, 2016, 10 (2), pp 1810–1819.

[31] Lademann J, Richter H, Teichmann A, Otberg N, Blume-Peytavi U, Luengo J, et al. Nanoparticles – an efficient carrier for drug delivery into the hair follicles. European Journal of Pharmaceutics and Biopharmaceutics. 2007;66(2):159–64.

[32] Bessar H, Venditti I, Fratoddi I, Benassi L, Vaschieri C, Azzoni P, et al. Functionalized gold nanoparticles for topical delivery of Methotrexate for the possible treatment of psoriasis. Colloids and Surfaces B: Biointerfaces. 2016, 141, 141–147.

[33] Zhang Q, Iwakuma N, Sharma P, Moudgil B, Wu C, McNeill J, et al. Gold nanoparticles as a contrast agent for in vivo tumor imaging with photoacoustic tomography. Nanotechnology. 2009;20(39):395102.

[34] Labouta HI, Liu DC, Lin LL, Butler MK, Grice JE, Raphael AP, et al. Gold nanoparticle penetration and reduced metabolism in human skin by toluene. Pharmaceutical Research. 2011;28(11):2931–44.

[35] Labouta H, El-Khordagui L, Schneider M. Could chemical enhancement of gold nanoparticle penetration be extrapolated from established approaches for drug permeation? Skin Pharmacology and Physiology. 2012;25(4):208–18.

[36] Fernandes R, Smyth NR, Muskens OL, Nitti S, Heuer-Jungemann A, Ardern-Jones MR, et al. Interactions of skin with gold nanoparticles of different surface charge, shape, and functionality. Small. 2015;11(6):713–21.

[37] Larese Filon F, Crosera M, Adami G, Bovenzi M, Rossi F, Maina G. Human skin penetration of gold nanoparticles through intact and damaged skin. Nanotoxicology. 2011;5(4):493–501.

[38] Liu DC, Raphael AP, Sundh D, Grice JE, Soyer HP, Roberts MS, et al. The human stratum corneum prevents small gold nanoparticle penetration and their potential toxic metabolic consequences. Journal of Nanomaterials. 2012;2012:7.

[39] Geusens B, Van Gele M, Braat S, De Smedt SC, Stuart MC, Prow TW, et al. Flexible nanosomes (SECosomes) enable efficient siRNA delivery in cultured primary skin cells and in the viable epidermis of ex vivo human skin. Advanced Functional Materials. 2010;20(23):4077–90.

[40] Prow TW, Grice JE, Lin LL, Faye R, Butler M, Becker W, et al. Nanoparticles and microparticles for skin drug delivery. Advanced Drug Delivery Reviews. 2011;63(6): 470–91.

[41] Zhu Y, Choe C-S, Ahlberg S, Meinke MC, Alexiev U, Lademann J, et al. Penetration of silver nanoparticles into porcine skin ex vivo using fluorescence lifetime imaging microscopy, Raman microscopy, and surface-enhanced Raman scattering microscopy. Journal of Biomedical Optics. 2015;20(5):051006.

[42] Gittard SD, Miller PR, Boehm RD, Ovsianikov A, Chichkov BN, Heiser J, et al. Multiphoton microscopy of transdermal quantum dot delivery using two photon polymerization-fabricated polymer microneedles. Faraday Discussions. 2011;149:171–85.

[43] Larson DR, Zipfel WR, Williams RM, Clark SW, Bruchez MP, Wise FW, et al. Water-soluble quantum dots for multiphoton fluorescence imaging in vivo. Science. 2003;300(5624):1434–6.

[44] Lo W, Ghazaryan A, Tso C-H, Hu P-S, Chen W-L, Kuo T-R, et al. Oleic acid-enhanced transdermal delivery pathways of fluorescent nanoparticles. Applied Physics Letters. 2012;100(21):213701.

[45] Boehm R, Miller P, Hayes S, Monteiro-Riviere N, Narayan R. Modification of microneedles using inkjet printing. AIP Advances. 2011;1(2):022139.

[46] Cheng S-H, Li F-C, Souris JS, Yang C-S, Tseng F-G, Lee H-S, et al. Visualizing dynamics of sub-hepatic distribution of nanoparticles using intravital multiphoton fluorescence microscopy. ACS Nano. 2012;6(5):4122–31.

[47] Semete B, Booysen L, Lemmer Y, Kalombo L, Katata L, Verschoor J, et al. In vivo evaluation of the biodistribution and safety of PLGA nanoparticles as drug delivery systems. Nanomedicine: Nanotechnology, Biology and Medicine. 2010;6(5):662–71.

[48] Johnston HJ, Semmler-Behnke M, Brown DM, Kreyling W, Tran L, Stone V. Evaluating the uptake and intracellular fate of polystyrene nanoparticles by primary and hepatocyte cell lines in vitro. Toxicology and Applied Pharmacology. 2010;242(1):66–78.

[49] Liang X, Grice JE, Zhu Y, Liu D, Sanchez WY, Li Z, et al. Intravital multiphoton imaging of the selective uptake of water-dispersible quantum dots into sinusoidal liver cells. Small. 2015;11(14):1711–20.

[50] Garrett NL, Lalatsa A, Uchegbu I, Schätzlein A, Moger J. Exploring uptake mechanisms of oral nanomedicines using multimodal nonlinear optical microscopy. Journal of Biophotonics. 2012;5(5–6):458–68.

[51] Chen A, Dogdas B, Mehta S, Haskell K, Ng B, Keough E, et al., editors. Quantification of Cy-5 siRNA signal in the intra-vital multi-photon microscopy images.

http://dx.doi.org/10.5772/63452

Engineering in Medicine and Biology Society (EMBC), 2012 Annual International Conference of the IEEE; 2012, San Diego, CA, USA.

[52] Loginova YF, Kazachkina NI, Zherdeva VV, Rusanov AL, Shirmanova MV, Zagaynova EV, et al. Biodistribution of intact fluorescent CdSe/CdS/ZnS quantum dots coated by mercaptopropionic acid after intravenous injection into mice. Journal of Biophotonics. 2012;5(11–12):848–59.

[53] Liang Y, Shilagard T, Xiao SY, Snyder N, Lau D, Cicalese L, et al. Visualizing hepatitis C virus infections in human liver by two-photon microscopy. Gastroenterology. 2009;137(4):1448–58.

[54] Boreham A, Kim T-Y, Spahn V, Stein C, Mundhenk L, Gruber A, et al. Exploiting fluorescence lifetime plasticity in FLIM: target molecule localization in cells and tissues. ACS Medicinal Chemistry Letters. 2011;2(10):724–8.

IntechOpen

IntechOpen

IntechOpen